

# Comparative Assessment of Sound Generated Using Laser-Induced Plasma

**Máté Szőke (VT), Christopher Bahr (NASA Langley), Louis Cattafesta (FSU),  
Karl-Stéphane Rossignol (DLR), Hiroki Ura (JAXA),  
Yang Zhang and Fernando Zigunov (FSU)**

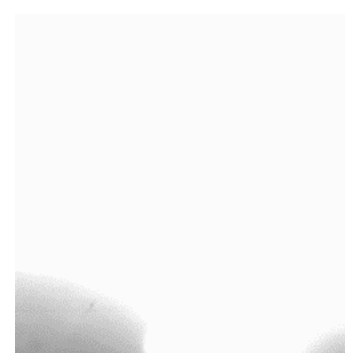
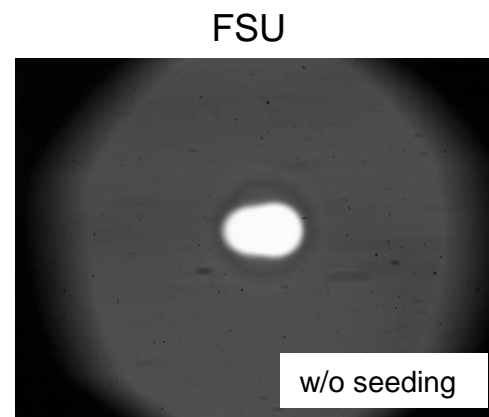
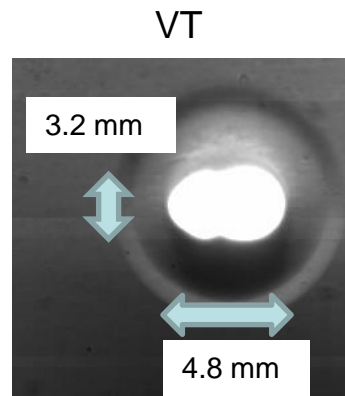
*Laser-induced plasma benchmark study  
3rd Hybrid Anechoic Wind Tunnel Workshop  
August 2021*

# Contents

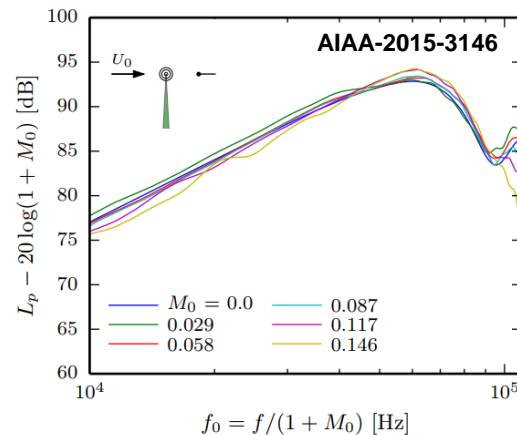
- **Overview** of laser-induced plasma and its properties
- Design of **laser-optical setup** (best practices)
- List of **facilities**
- List of **experimental setups**
- **Comparative study** of acoustic signatures
- **Health and safety** measures
- **Application examples**

# Overview of laser-induced plasma (LIP)

- **Properties of LIP**
  - **Tight-focusing of laser beam** results in **plasma formation** once a sufficiently high energy density is reached
  - Also generates an **acoustic source**
  - Source is **well localized**
  - **Repeatable**
  - **Good temporal characteristics** (initially supersonic propagation)
  - **Good omnidirectionality** (no flow)
  - With flow: convection effect (**Doppler shift**)
    - **Can be accounted for** (AIAA-2015-3146)
  - **Suitable for high-frequency analysis** (2-100 kHz) + good **signal-to-noise ratio** (loud)
- Laser-optical requirements primarily rely on **laser head (PIV)** and **secondarily on optics** (also cost-wise)
- Observed **waveform depends on instrumentation** hence this collaborative effort.

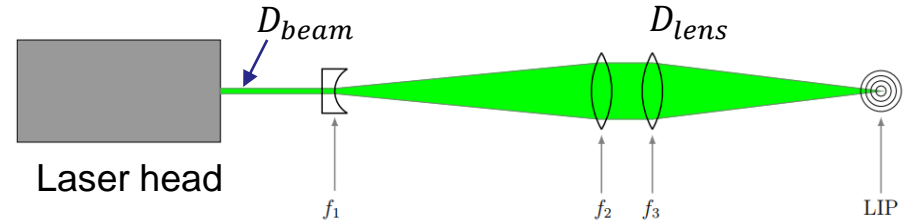


200 kFrames/sec (5  $\mu$ s)  
1.62  $\mu$ s exposure time  
Timespan: 100  $\mu$ s



# Laser-optical design

- Using a **beam expander** plus **focusing optics**
- **Laser properties:** energy per pulse, pulse width (ns), beam: diameter ( $D_{beam}$ ), area, divergence (mrad), wavelength ( $\lambda$ ).
- Determine **focusing optics** from WTL test section size ( $f_3$ )
- Calculate **magnifying power** (MP) to select beam expander
  - **Image lens** focal length ( $f_1$ )
- Calculate "**spot size**" ( $\phi_{spot}$ )
  - Diffraction, and **aberration** limits (aspherical lens)
  - **Minimize**  $f_3/D_{lens}$  (i.e., f-number) for tight-focusing
  - **Laser beam quality** ( $M^2$ )
- Calculate **energy density** in spot
  - Exceed threshold\* of  $3.5 \cdot 10^{16} \text{ W/m}^2$

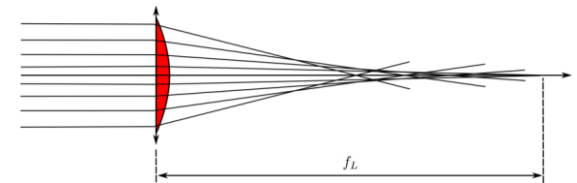


$$MP = \frac{D_{beam}}{D_{lens}} = -\frac{f_2}{f_1} \rightarrow f_1 = -\frac{f_2}{MP}$$

$$\phi_{Spot\ Size} = \phi_{Diffraction} + \phi_{Aberration} = \frac{4\lambda M^2 f}{\pi D} + \frac{kD^3}{f^2}$$

<https://www.edmundoptics.com/knowledge-center/application-notes/lasers/beam-expanders/>

Primary limitation: spherical aberration  
~O(1) greater than diffraction (VT, DLR)



\*Phuoc, T.X.: Laser spark ignition: experimental determination of laser-induced breakdown thresholds of combustion gases. *Opt. Commun.* 175(4), 419–423 (2000)

# Laser-optical arrangements

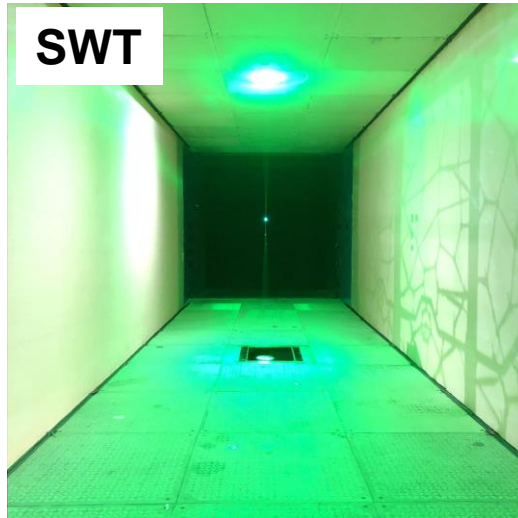
OPTICAL/PLASMA PROPERTIES	VT SWT	NASA Langley QFF	DLR (AWB)	FSU	JAXA
Focal length	1200 mm	~500 mm (approx.)	500 mm	500 mm	1200 mm
Laser head	Quantel Evergreen 200	New Wave Gemini	New Wave Gemini	Quantel Evergreen 200	Thales SAGA 230
Laser energy ( $E_L$ )	200 mJ	120 mJ	120 mJ	200 mJ	1250 mJ
Laser pulse width	10 ns	3-5 ns	3-5 ns	10 ns	8 ns
Laser stability (% RMS)	2%	3.5%	3.5%	2%	1.2%
Wavelength	532 nm	532 nm	532 nm	532 nm	532 nm
Beam diameter (nominal)	6.35 mm	5 mm	5 mm	6.5 mm	13 mm
Laser repetition rate used	5/second	5/second	10/second	2/second	10/second
Calculated beam energy density at focal point ( $W/m^2$ )	1.70E12	N/A	6.9E13	3.4E12	1.5E12 @ 120 mJ 4.8E12 @ 400 mJ (beam $E_L$ measured)
Optical setup expenses	\$3000 - 2 pcs of Celestron AVX 6" telescopes (2x\$1500) \$200 - hardware \$1200 - smaller optics (f=200 mm)	\$3500 - lenses and lens holders \$160 - photodetector \$550 - glass panel for use in QFF sidewall	\$1200	\$920 - beam expander (\$600) + converging lens (\$120) + hardware (\$200) + Dantec beam expander (cost unknown)	N/A
M <sup>2</sup> number used	20	N/A	30	6	9.6
front lens f number	8		12.5	4	8

# Facilities overview

	VT SWT	NASA Langley QFF	DLR (AWB)	FSU	JAXA
<b>Test section size (ft &amp; m)</b>	6' x 6' x 24' 1.83 m x 1.83 m x 7.3 m	2' x 3' x 6' 0.6 m x 0.91 m x 1.83 m	2.6' x 3.9' x 9.8' 0.8 m x 1.2 m x 3.0 m	3' x 4' x 10' 0.91 m x 1.22 m x 3 m	6.6' x 6.6' x 13.1' 2 m x 2 m x 4 m
<b>Flow speed range</b>	20 - 70 m/s	0 - 58 m/s	0 - 60 m/s	0 - 70 m/s	0-67 m
<b>Reynolds number (max)</b>	5 million/m	4 million/m	4 million/m	5 million/m	4.4 million/m
<b>Typical test object size (e.g., chord)</b>	0.6 - 0.9 m	0.2 - 0.5 m	0.2 - 0.5 m	0.2 - 0.5 m	1 m
<b>Observer angles: polar (defined wrt. Mach vector)</b>	40-140 deg	45-135 deg	~ +/- 180 deg		~ 45 - 135 deg
<b>Observer angles: azimuth</b>	~ +/- 30 deg	~ +/- 30 deg	~ +/- 60 deg		+/- 30 deg
<b>Frequency range of interest</b>	250 Hz - 20 kHz	~ 1 kHz - 80 kHz (5 - 50 nom.)	~ 1 kHz - 80 kHz (5 - 50 nom.)	250 Hz - 20 kHz	315 Hz - 80 kHz
<b>Tunnel type(s):</b>	Kevlar walls	Open-jet, Kevlar panel	Open-jet	Open-jet, Kevlar panel, glass panel	Kevlar walled test section Solid wall Gust wind test section Open jet test section

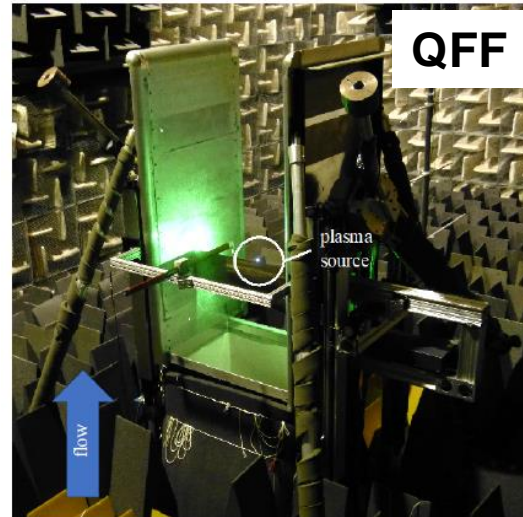
# Facilities I.

Kevlar walls



6' x 6' x 24'  
(1.83 m x 1.83 m x 7.3 m)  
f = 1200 mm

Open-jet



2' x 3' x 6'  
(0.6 m x 0.91 m x 1.83 m)  
f ≈ 500 mm

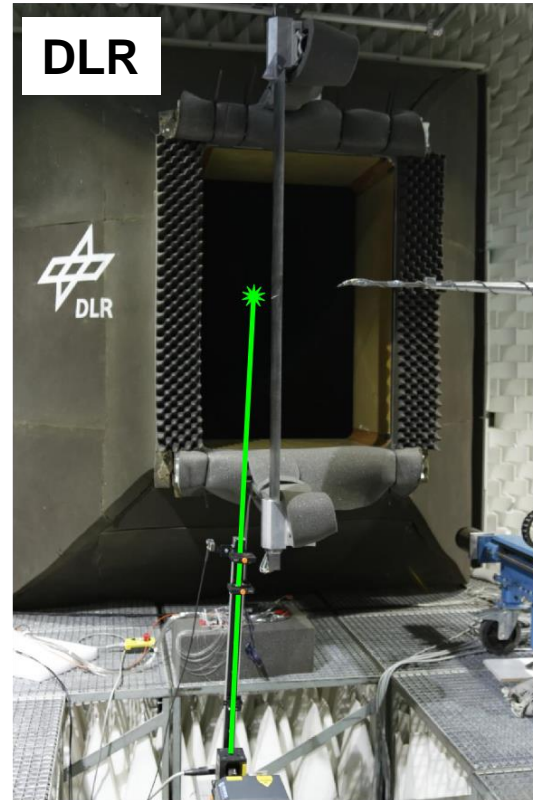
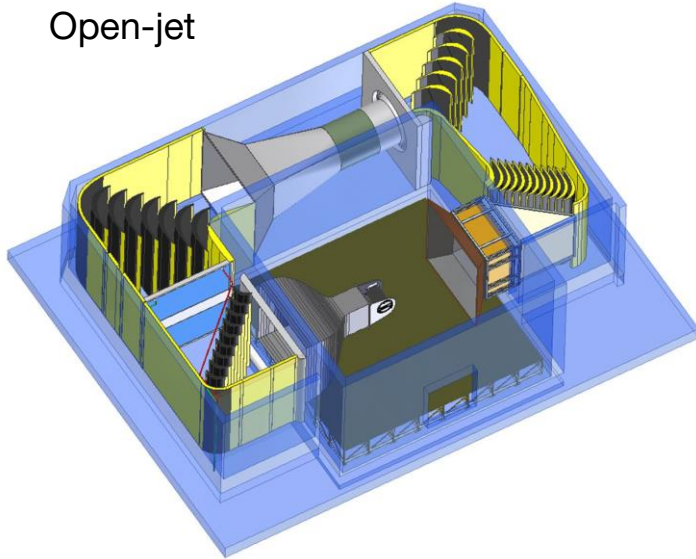
Kevlar panel



AIAA-2020-1253

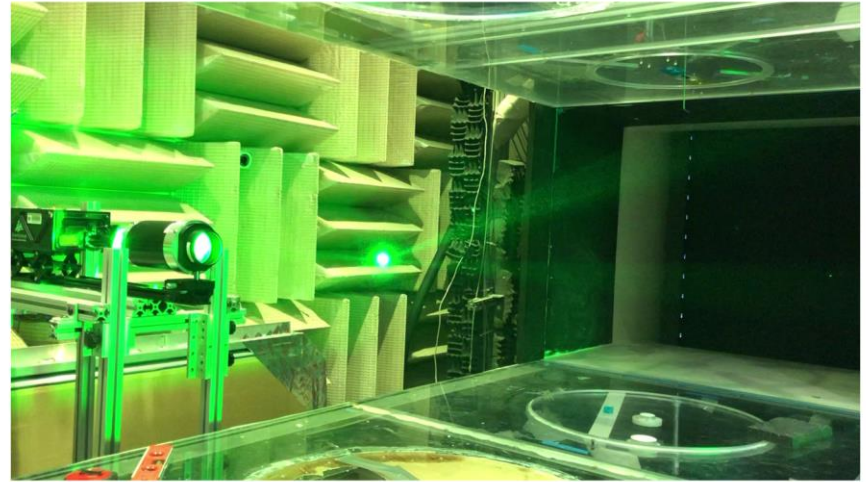
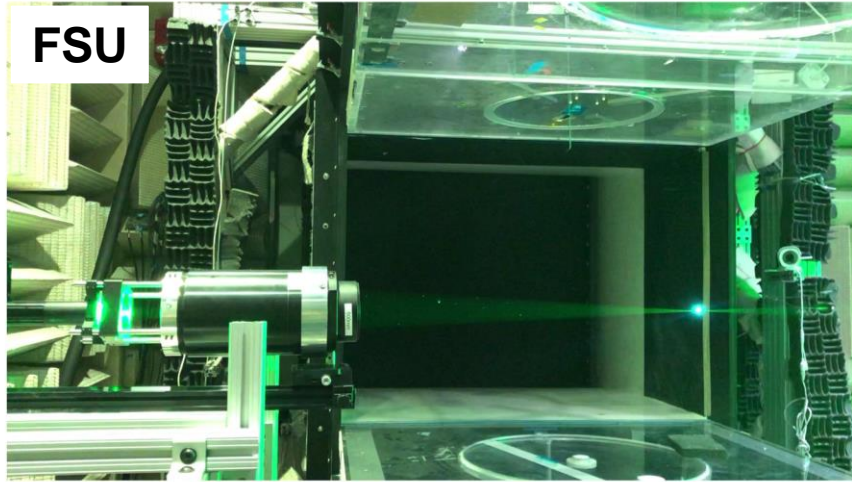
# Facilities II.

Facility: **AWB**  
2.6' x 3.9' x 9.8'  
(0.8 m x 1.2 m x 3.0 m)  
 $f \approx 500$  mm  
Open-jet



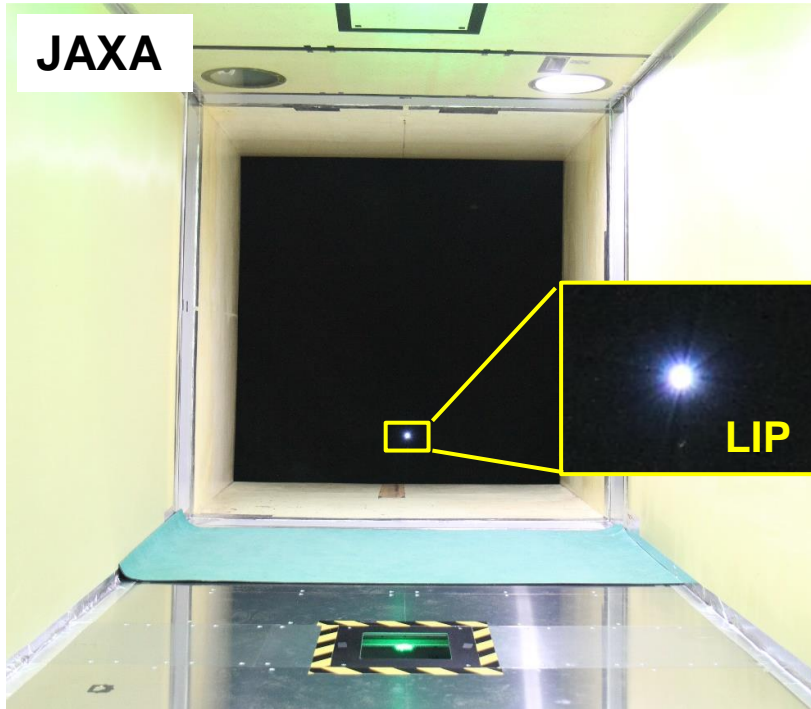


# Facilities III.



3' x 4' x 10'  
(0.91 m x 1.22 m x 3 m)  
f = 500 mm  
Kevlar walls

# Facilities IV.



**JAXA**

6.6' x 6.6' x 13.1'  
(2 m x 2 m x 4 m)  
f = 1200 mm  
Kevlar walls

# Instrumentation

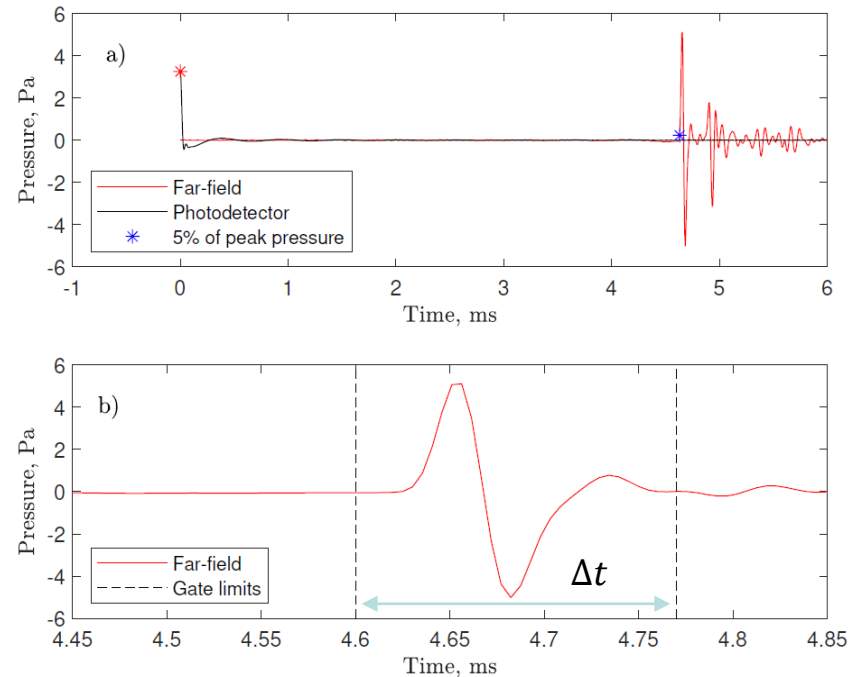
INSTRUMENTATION	VT SWT	NASA Langley QFF	DLR (AWB)	FSU	JAXA
<b>Microphones available</b>	GRAS 40 PH (50 Hz - 20 kHz)	B&K 4138 (6.5 Hz - 140 kHz); B&K 4938 (4 Hz - 70 kHz)	GRAS 40 DP (6.5 Hz - 140 kHz)	GRAS 40BE (4 Hz - 80 kHz); B&K 4958 (10 Hz - 20 kHz)	B&K 4939 (4 Hz - 100 kHz),
<b>DAQ system</b>	General Standards Corp. PCIe-16A64SSC	NI PXI 6120; NI PXIe 4480; NI PXI-5122	GBM Viper 48 Channels (3X)	NI PXI-1045; NI PXI-4462	NI PXI-4462
<b>Sampling rate</b>	192 kS/s	250 kS/s (800 nom.); 1.25 MS/s (20 streaming); 100 MS/s	250 kS/s	204.8 kS/s	204.8 kS/s
<b>Laser emission detection</b>	Photodetector signal	Photodetector signal, Q-switch	Q-switch	Photodetector signal	N/A
<b>Filters</b>	Low-pass 20kHz	Low-pass 100 kHz		Low-pass 80 kHz	
<b>Flow speed range</b>	0-70 m/s	0-58 m/s	0-65 m/s	0-70 m/s	0-65 m/s
<b>LIP to observer distance</b>	ranging between 1.6 m and 2.5 m	variable within several meters	variable within several meters	< 2 m	1.865 m

# Comparative study of acoustic signatures

- **Ensemble-averaged time signature** of the pressure wave for a single microphone (without flow)
- **Fourier transform** of the gated ensemble-averaged pressure wave signal of a single microphone (without flow)
- **Uncertainty analysis** of LIP arrival time and LIP sound level

# Processing steps – Current study

- **High-pass filtering** at 1 kHz to remove facility-dependent **background noise**
- **Block** formation (laser emission at  $t = 0$  s), **LIP** sound **identification** (reject if needed)
- **Arrival time** ( $\tau_a$ ) calculation: given % threshold of peak pressure
- **Normalizing** with peak pressure
  - $\hat{p} = p/p_{max}$
- **Gating** ( $\hat{p}_G$ ), **windowing** (25% Tukey), **zero padding** (0.1s)
- **Fourier** transform
- **Sound energy** calculation
  - $E = \frac{1}{\Delta t} \int \hat{p}_G^2(t) dt$
- **Uncertainty** calculation (95% confidence)
  - $\delta_\tau = 1.96 \cdot \text{std}(\tau_a)$
  - $\delta_p = 1.96 \cdot \text{std}(10 \log_{10} E)$



# Comparative study of acoustic signatures

- **Ensemble-averaged time signature** of the pressure wave for a single microphone (without flow)
- Fourier transform of the gated ensemble-averaged pressure wave signal of a single microphone (without flow)
- Uncertainty analysis of LIP arrival time and LIP sound level

# Time signature of pressure wave I.

## Virginia Tech data

GRAS 40PH 1/4", with gridcap

LIP-to-mic distance: 1671 mm

$f_s = 192$  kS/s

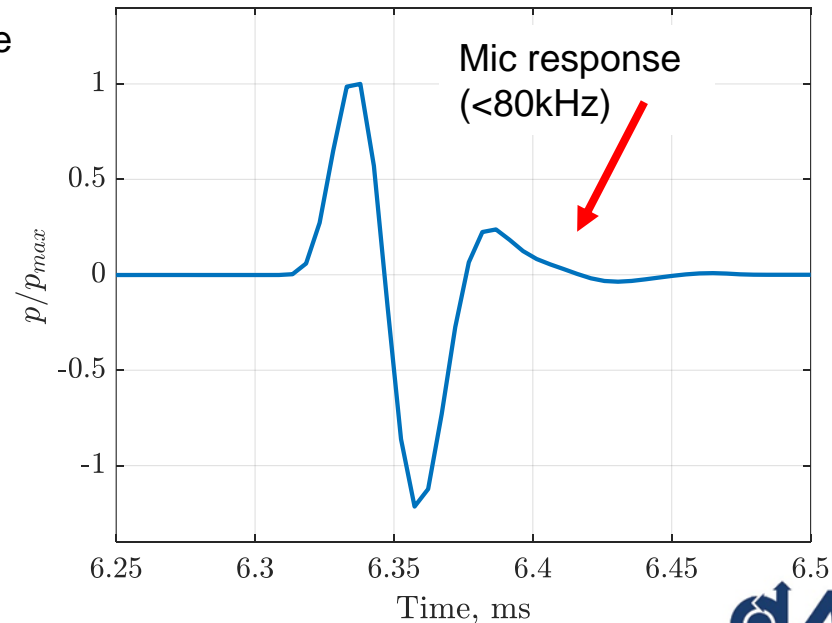
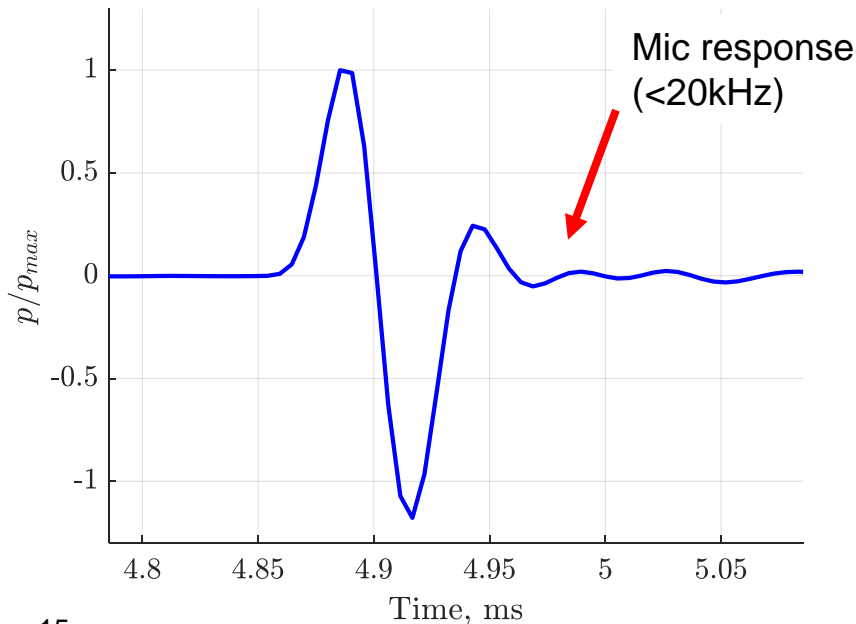
## Evergreen laser heads

## Florida State Uni data

GRAS 40BE 1/4", with gridcap

LIP-to-mic distance: 2150 mm

$f_s = 204.8$  kS/s



# Time signature of pressure wave II.

## DLR data

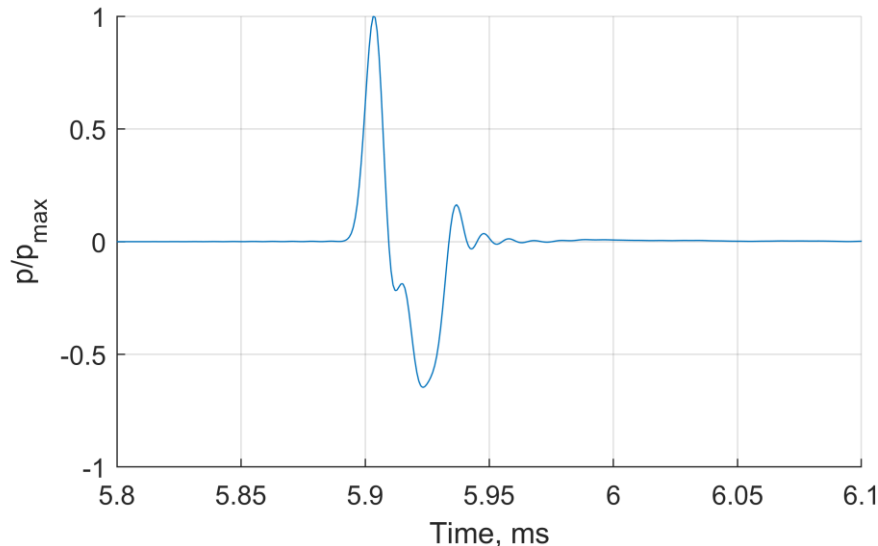
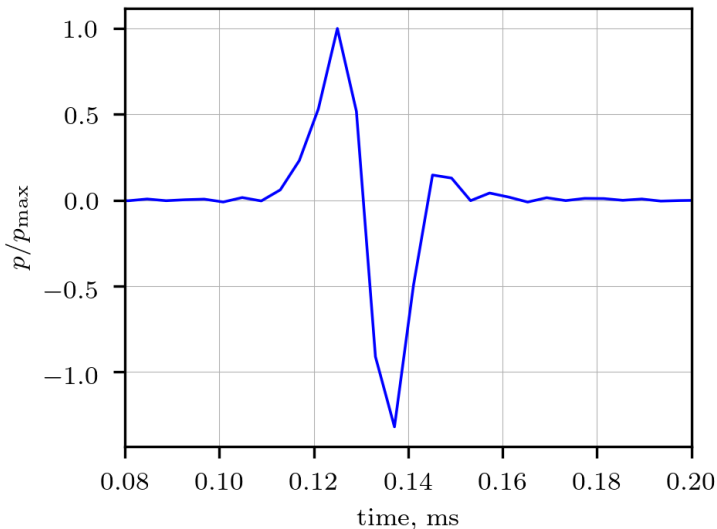
GRAS 40DP 1/8", with gridcap  
LIP-to-mic distance: 1000 mm  
 $f_s = 250$  kS/s

## New Wave laser heads

$f_s \approx 200$  kS/s is at the lower end  
Time domain is more sensitive for  $f_s$

## NASA Langley QFF data

B&K 4138 1/8", with gridcap  
LIP-to-mic distance: 2019 mm  
 $f_s = 1.25$  MS/s





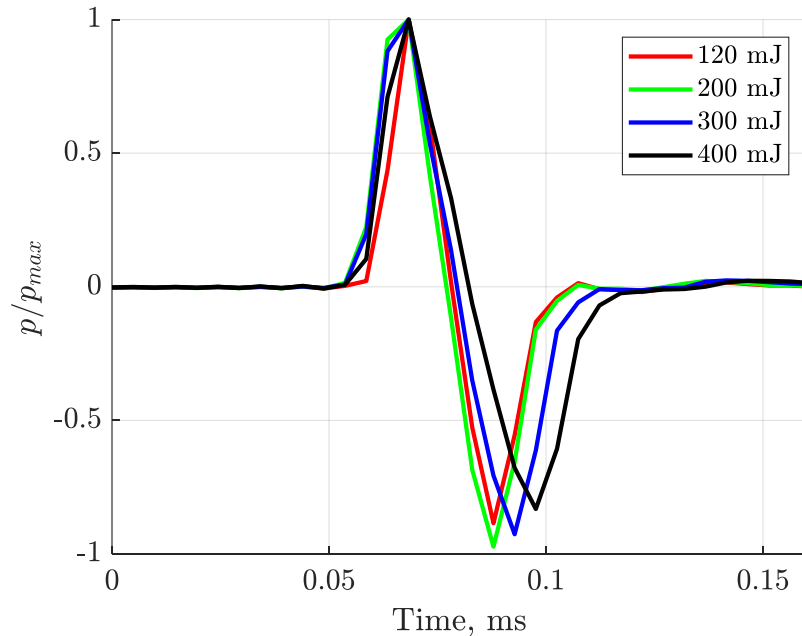
# Time signature of pressure wave III.

## JAXA data

B&K 4939 1/4", without gridcap

LIP-to-mic distance: 1865 mm

$f_s = 204.8$  kS/s



- **Pressure front** collapses relatively well
- **Effect of laser power** is more significant in the second half of the signal
- The **time difference between the positive and negative peaks increases**
- **Further investigations** might shed light on (a) initial non-linear propagation properties and (b) plasma "lifetime"

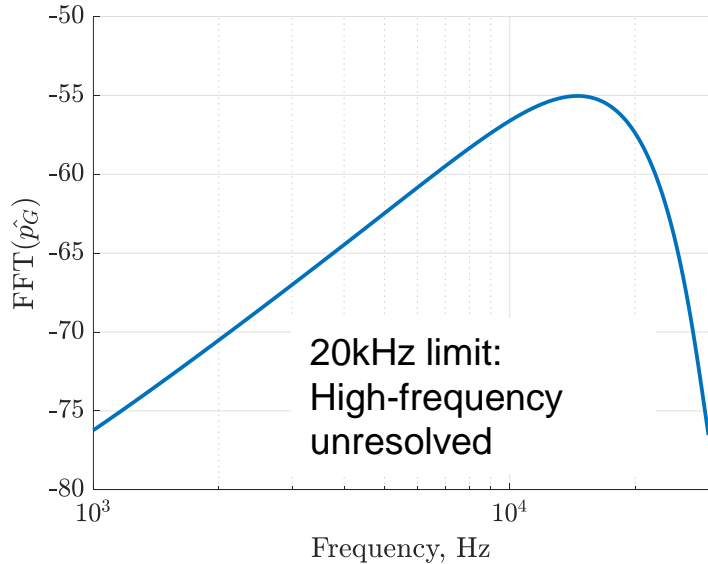
# Comparative study of acoustic signatures

- Ensemble-averaged time signature of the pressure wave for a single microphone (without flow)
- **Fourier transform** of the gated ensemble-averaged pressure wave signal of a single microphone (without flow)
- Uncertainty analysis of LIP arrival time and LIP sound level

# Frequency domain I.

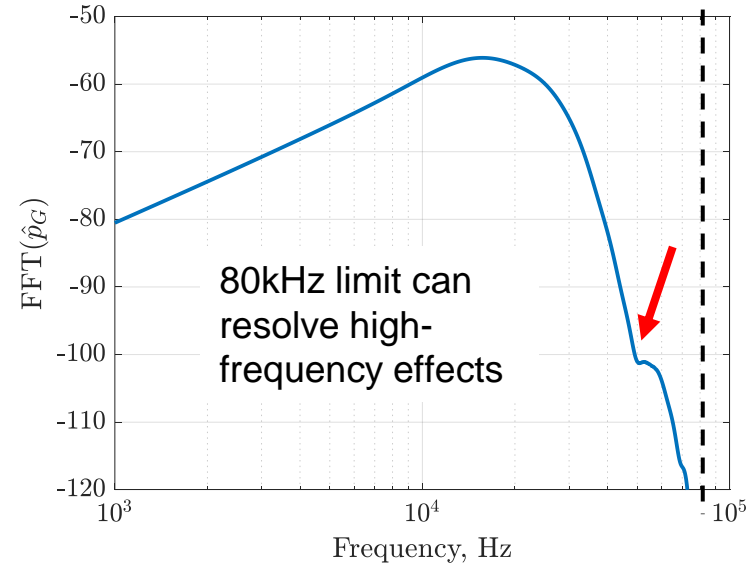
## Virginia Tech data

GRAS 40PH 1/4" (50 Hz – 20 kHz)  
1 kHz high-pass, 20 kHz anti-alias  
200 mJ Evergreen laser



## Florida State Uni data

GRAS 40BE 1/4" (4 Hz – 80 kHz)  
1 kHz high-pass, 80 kHz low-pass  
200 mJ Evergreen laser



High-frequency effects  $\neq$  nearfield violation

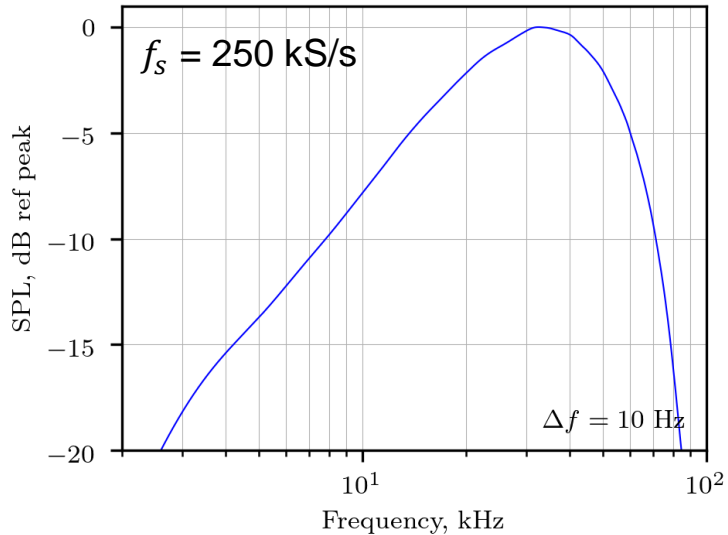
# Frequency domain II.

## DLR data

GRAS 40DP 1/8" (6.5 Hz – 140 kHz)

2 kHz high-pass, 100 kHz low-pass

120 mJ New Wave Gemini laser



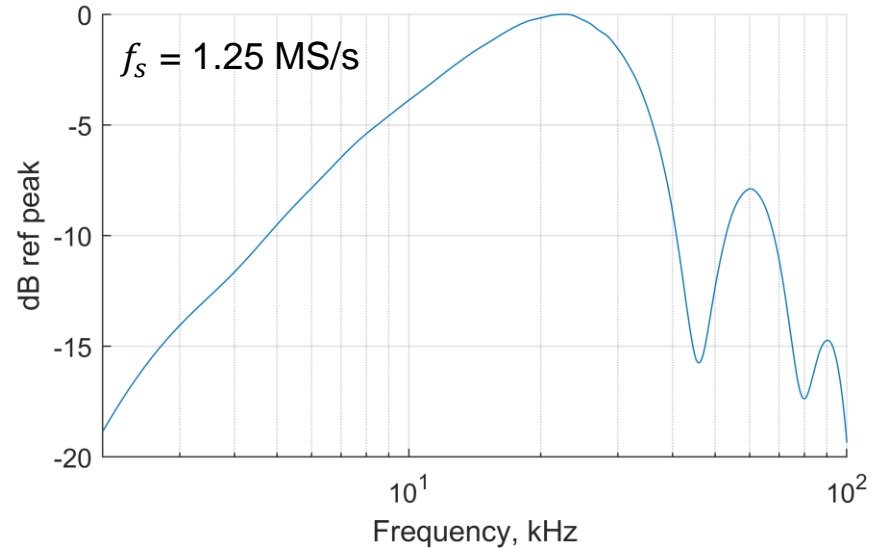
$f_s \approx 200$  kS/s seems to suffice for frequency domain analysis  
The acoustic signatures of the two LIP formations may differ

## NASA Langley QFF data

B&K 4138 1/8" (6.5 Hz – 140 kHz)

2 kHz high-pass, 100 kHz low-pass

120 mJ New Wave Gemini laser



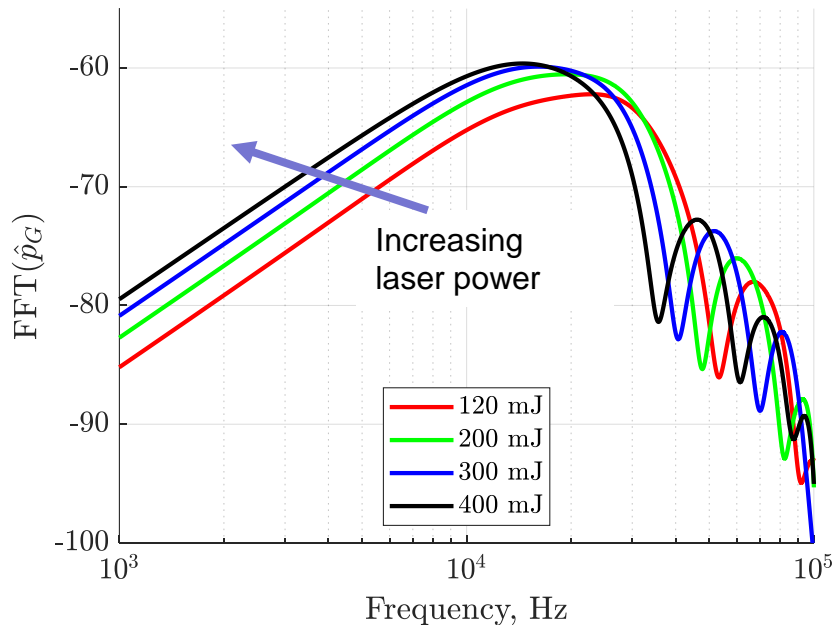
# Frequency domain III.

## JAXA data

B&K 4939 1/4" (4 Hz – 100 kHz)

1 kHz high-pass

Thales SAGA 230 laser (1250 mJ)



- **Frequency** response remains **linear below 10 kHz**, while levels increase with laser power (5 dB)
- High-frequency effects shift to **lower frequencies** with **increasing laser power**

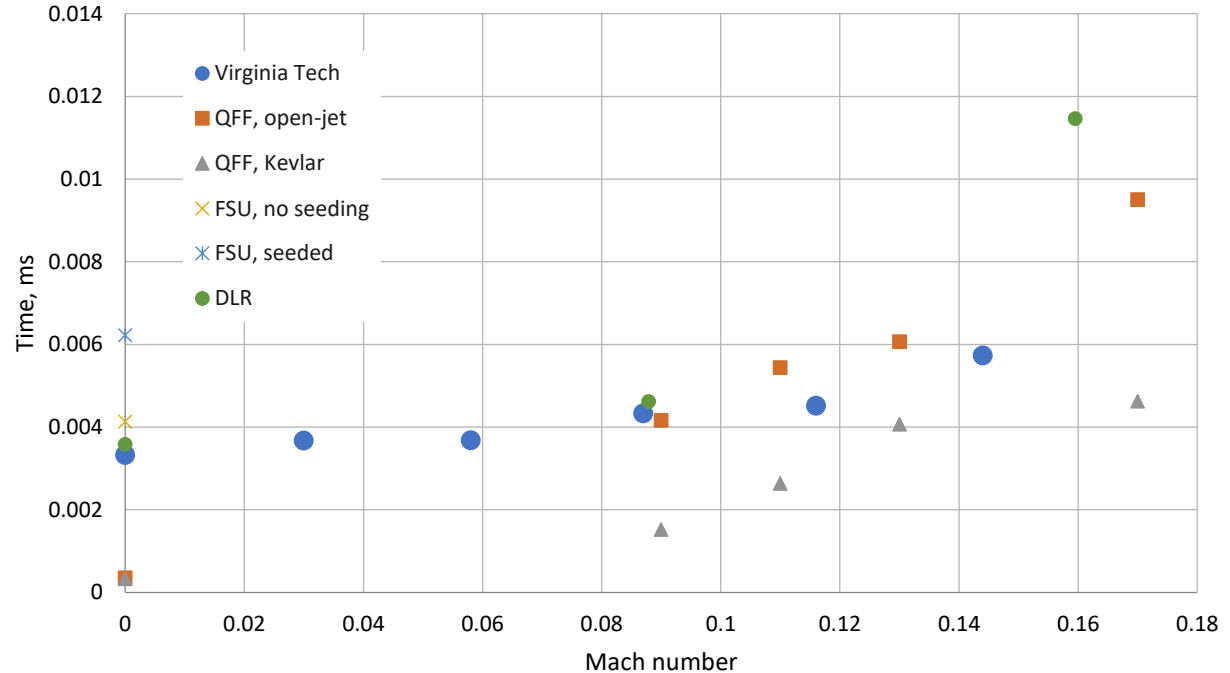
# Comparative study of acoustic signatures

- Ensemble-averaged time signature of the pressure wave for a single microphone (without flow)
- Fourier transform of the gated ensemble-averaged pressure wave signal of a single microphone (without flow)
- **Uncertainty analysis of LIP arrival time and LIP sound level**

# Uncertainty analysis I.

- **Arrival time uncertainty**
  - $\delta\tau = 1.96 \cdot \text{std}(\tau_a)$
- **Limit:**  
 $1/f_s = 0.004\text{-}0.005$  ms  
(except for QFF:  
 $1/f_s = 0.0008$  ms)
- **Somewhat below limit** (thanks to linear interpolation to find  $\tau_a$ )
- **Uncertainty increases with flow speed:** unsteady, turbulence effects
- **Kevlar shows reduced flow effects compared to open-jet**
- **PIV seeding increases temporal uncertainty (FSU)**
  - LIP location becomes uncertain:  
 $\pm 2$  mm ( $\approx \pm 0.006$  ms)

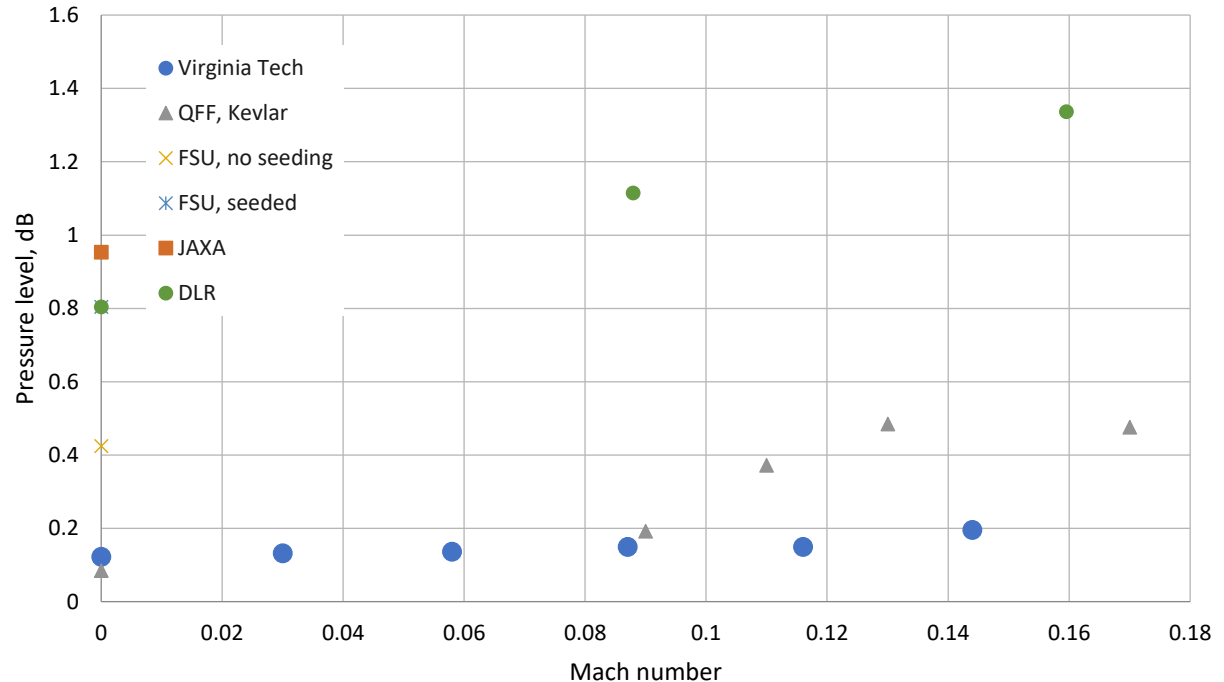
Arrival time uncertainty



# Uncertainty analysis II.

Pressure level uncertainty

- **Pressure level uncertainty**
  - $\delta_p = 1.96 \cdot \text{std}(10\log_{10}(E))$
- **At  $M = 0$ , instrumentation limited**
- **Increases with flow speed**
- **QFF vs. VT results with flow suggest insufficient temporal resolution ( $f_s \approx 200\text{kS/s}$ ) to resolve unsteady effects below  $M=0.1$**
- **PIV seeding increases pressure uncertainty, too**





# Uncertainty analysis III.



## Pressure level uncertainty

$\delta_p = 1.96 \cdot \text{std}(10\log_{10}(E))$

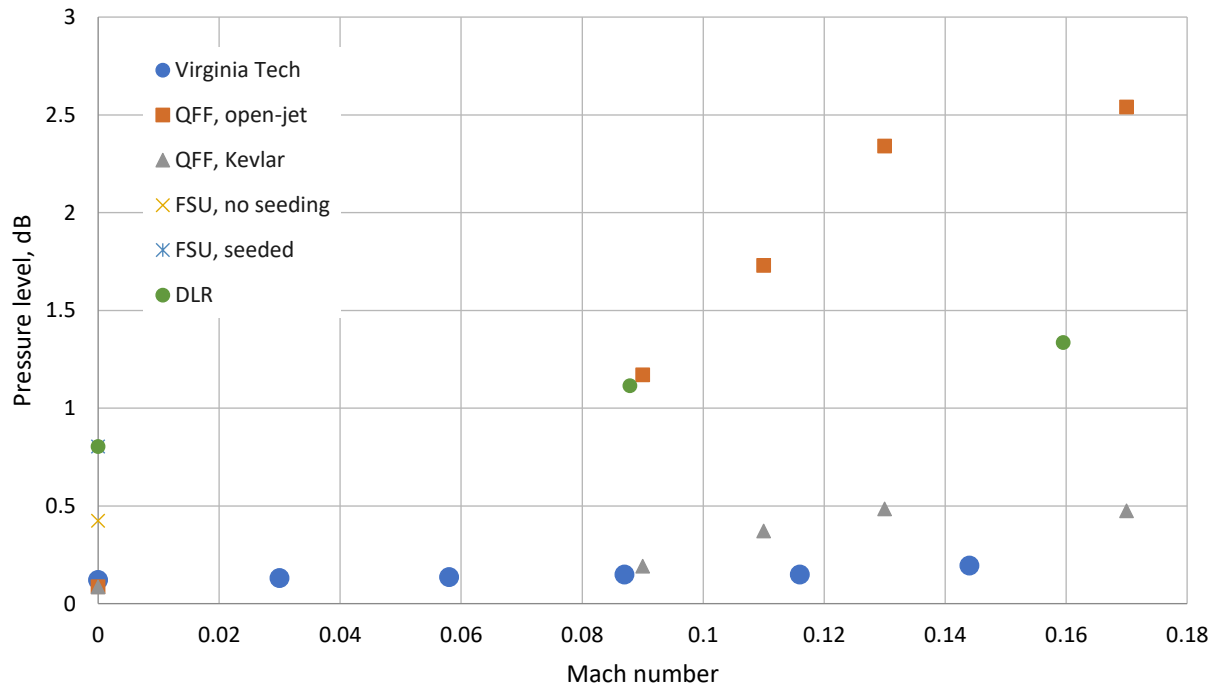


**Pressure level uncertainty is dramatically higher for open-jet configuration** (almost by a factor of 5)



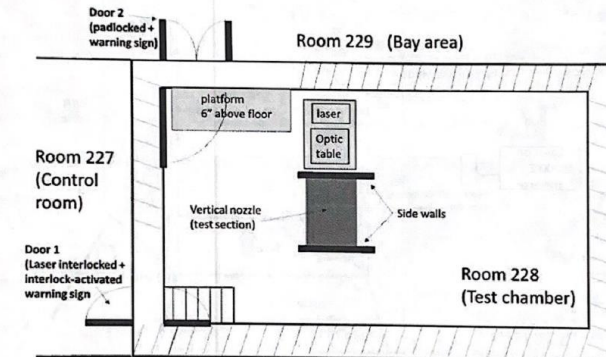
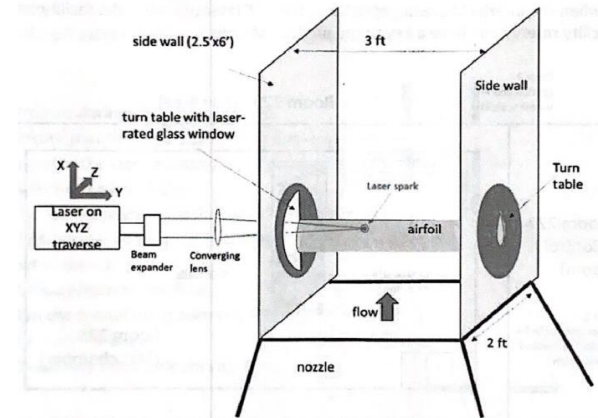
Kevlar + BL and sound interaction is significantly weaker than shear-layer and sound interaction

Pressure level uncertainty



# Health and safety (H&S) measures (QFF, DLR, VT)

- Approached H&S as a **PIV experiment** (laser safety)
- **Personnel exposure**
  - Participants must take **laser safety training** prior to testing
  - **Minimize personnel** in chamber
  - Wear laser safety **glasses at all times**
  - **Hearing protection** was not required
- **Experimental setup**
  - **Warning signs** and **lights** tied to laser interlock
  - Optical **barricades**, **CCTV** camera, microphone
  - **Cover and clear laser beam path**, verify sufficient beam divergence for “safe” reflections w.r.t. ablation, combustion when beam is not covered
  - Develop **remote operation of laser**
  - **Interlocks** tie access door to laser power (open door = power cut off)
  - **Padlocked auxiliary doors** – only approved operators or facility coordinator/safety head can lock/unlock these
  - **Always keep the area around the focal point (LIP) clear**

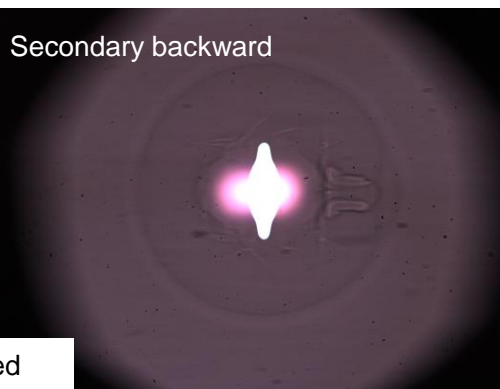
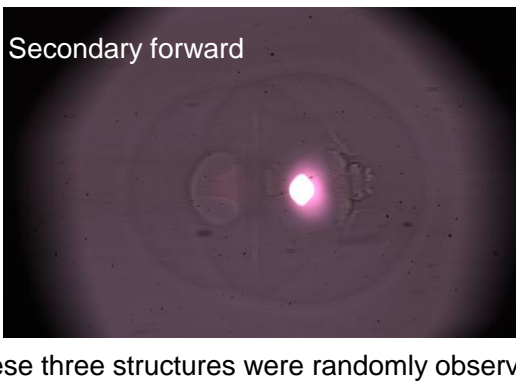
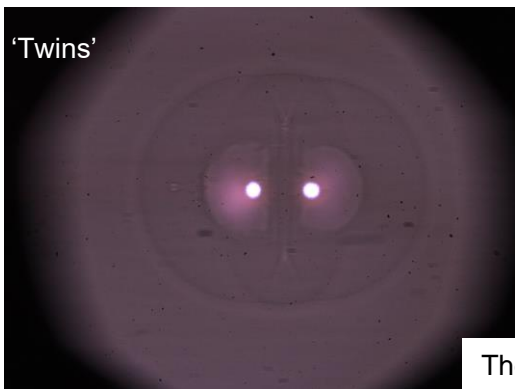
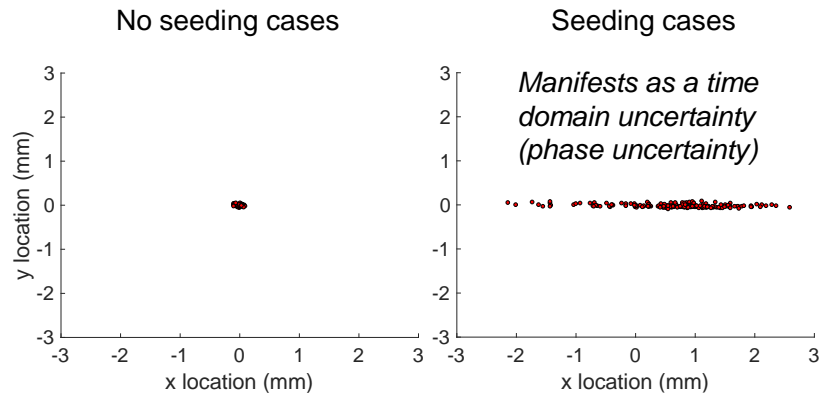
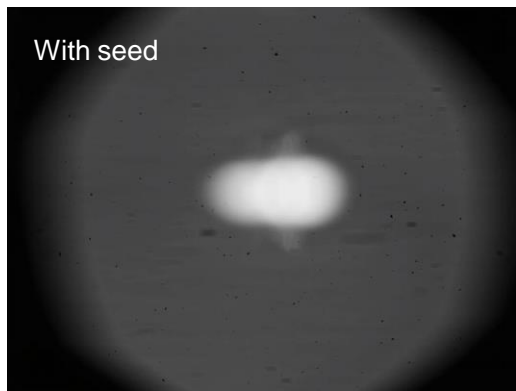
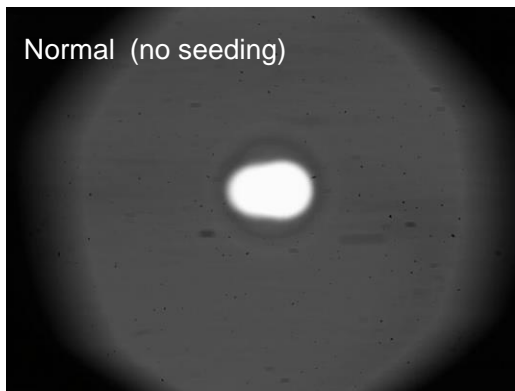


26 see Appendix for extra details on H&S

# Application examples

# Shadowgraph analysis of seeding effect (FSU)

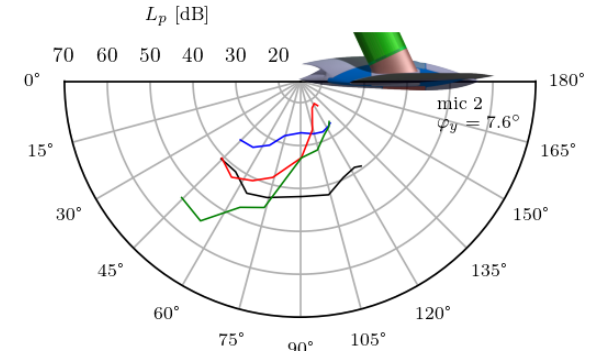
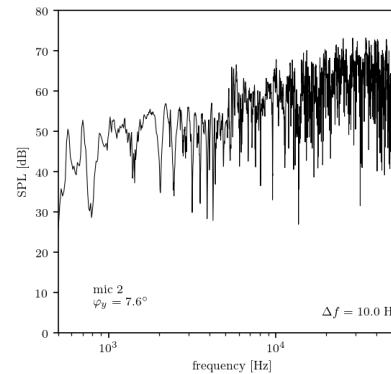
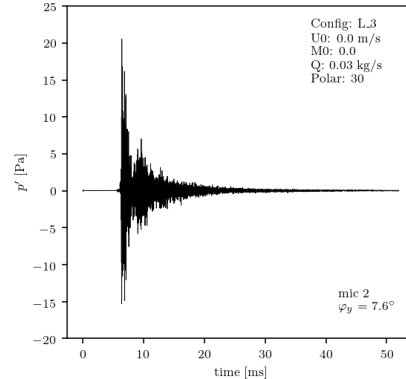
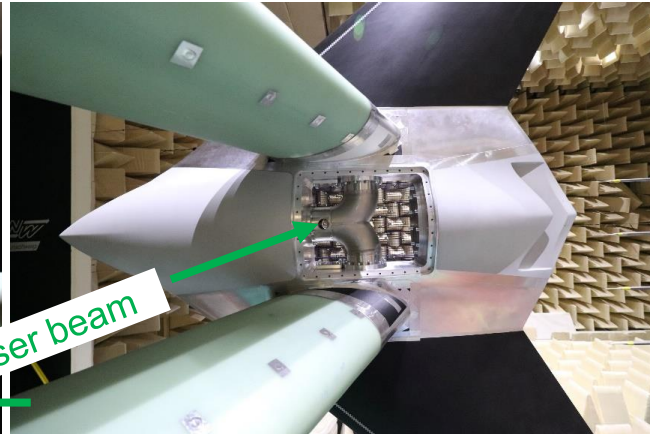
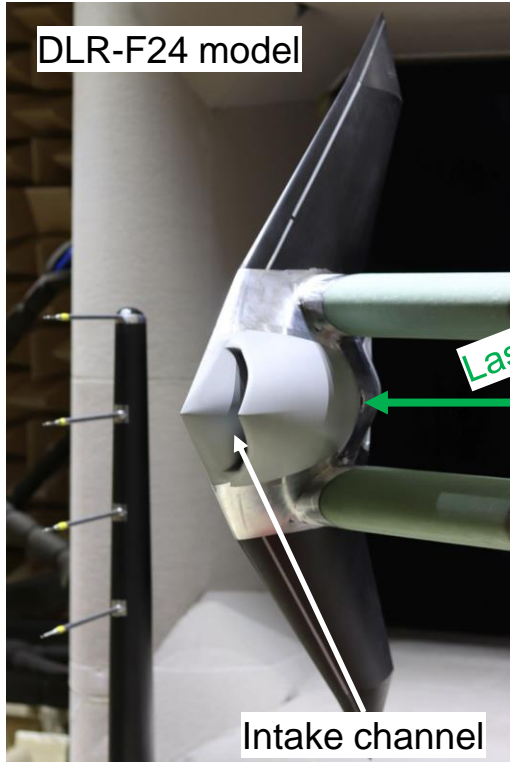
## Sparks without and with PIV seeding



These three structures were randomly observed

# Application examples: DLR

Triggering acoustic channel modes under no flow conditions (DNW-NWB, 2021)



Config: L3  
 $U_0$ : 0.0 m/s  
 $M_0$ : 0.0  
 $Q$ : 0.03 kg/s  
 Polar: 30

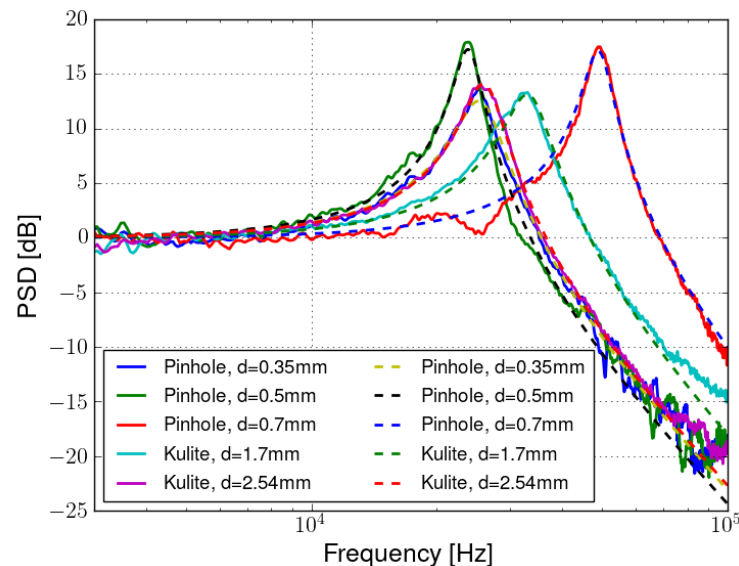
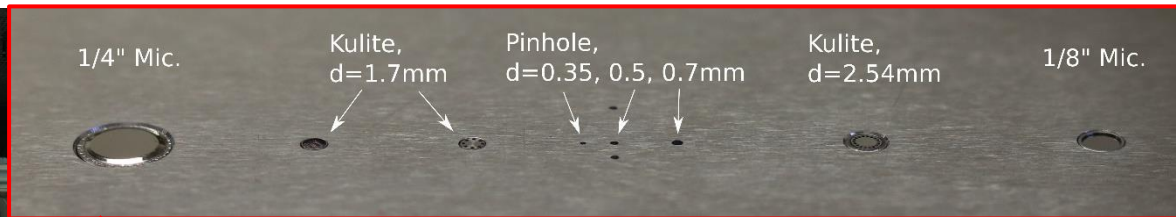
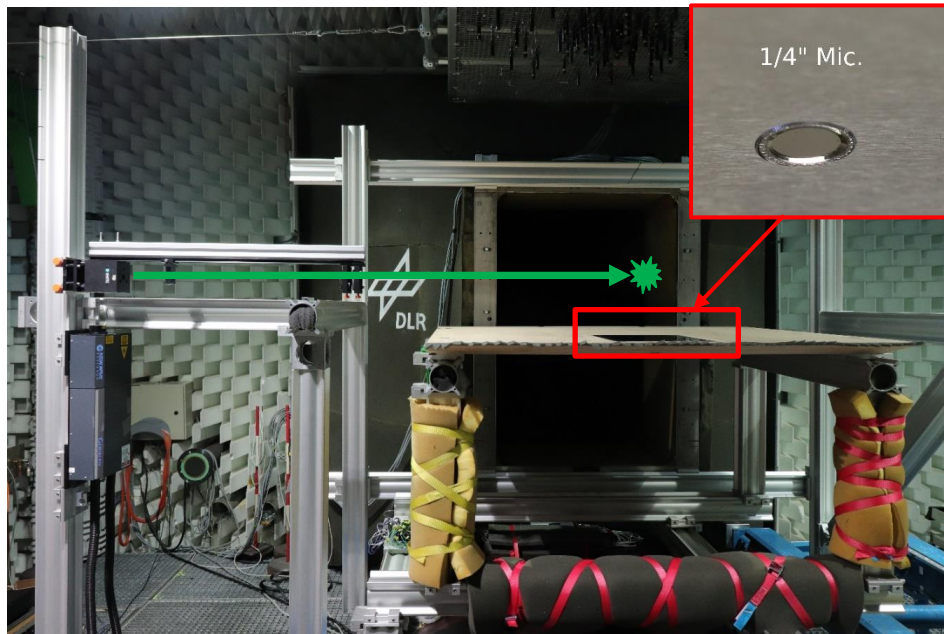
$f =$

- 1007.08 Hz
- 2502.44 Hz
- 5004.88 Hz
- 10009.77 Hz

Currently validating against CAA results. Implementation of LIP in CAA is straightforward.

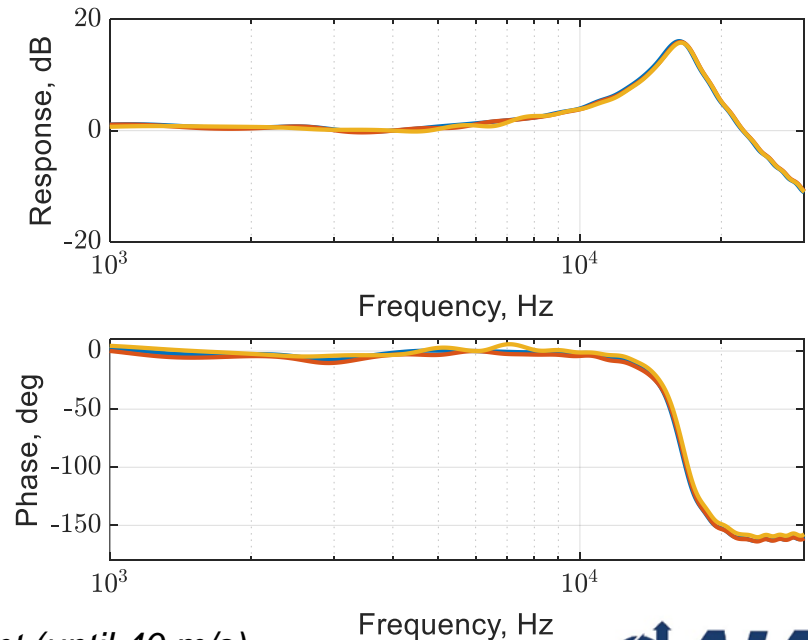
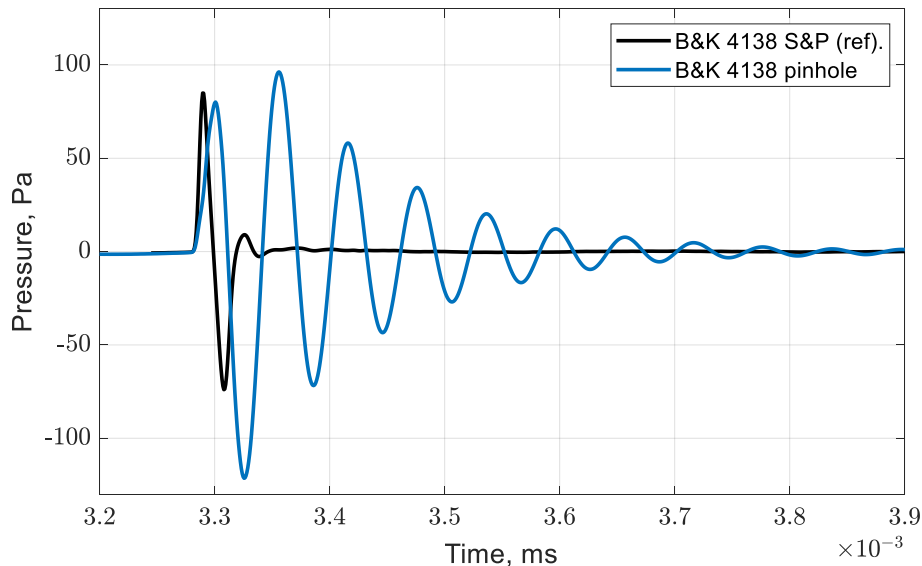
# Application examples: DLR

Calibration of flush-mounted microphones using a reference microphone (AWB, 2019)



# Application examples: VT

Calibrating a B&K 4138 (1/8") flush-mounted **pinhole microphone** at high-frequencies using another flush-mounted B&K 4138 (1/8") as a reference (gridcap) microphone.

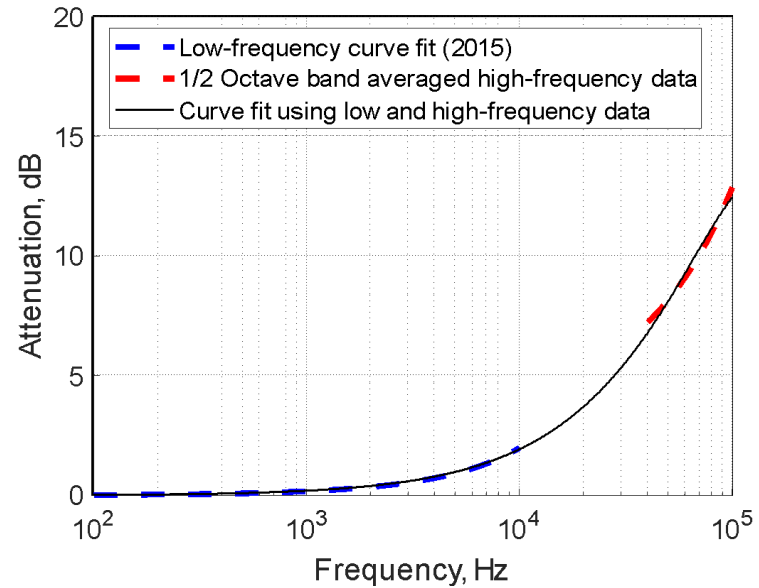
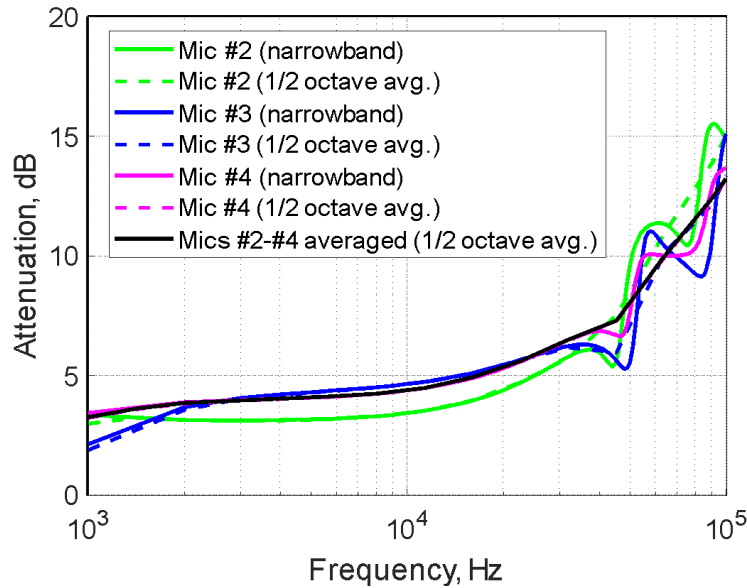


*Highly repeatable, flow-independent (until 40 m/s)*

# Application examples: VT

Measuring **Kevlar transmission loss at high-frequencies** using two B&K 4138 (1/8") microphones: (a) one inside the test section and (b) one behind the Kevlar.

*Comparing a given LIP formation across identical types of microphone pairs.*





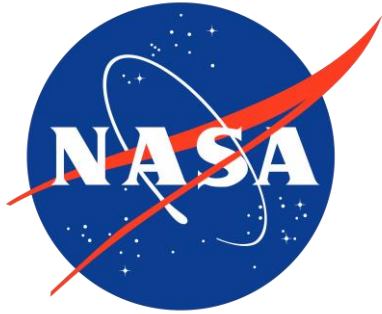
## ➤ **Potential future work**

- Effects of laser power on acoustics & quantifying laser power level at the focal point
- Instrumentation effects (microphones used, incidence angle, sampling rate etc).
- Convection effect on plasma formation (high-speed shadowgraph)

## ➤ **Potential discussion items**

- What % of threshold to use for detecting arrival time?
- Alternative windowing options for data processing?
- Is there an interest in performing a benchmark analysis of LIP?

Thank you!



AMERICAN INSTITUTE OF  
AERONAUTICS AND ASTRONAUTICS



VIRGINIA  
TECH.



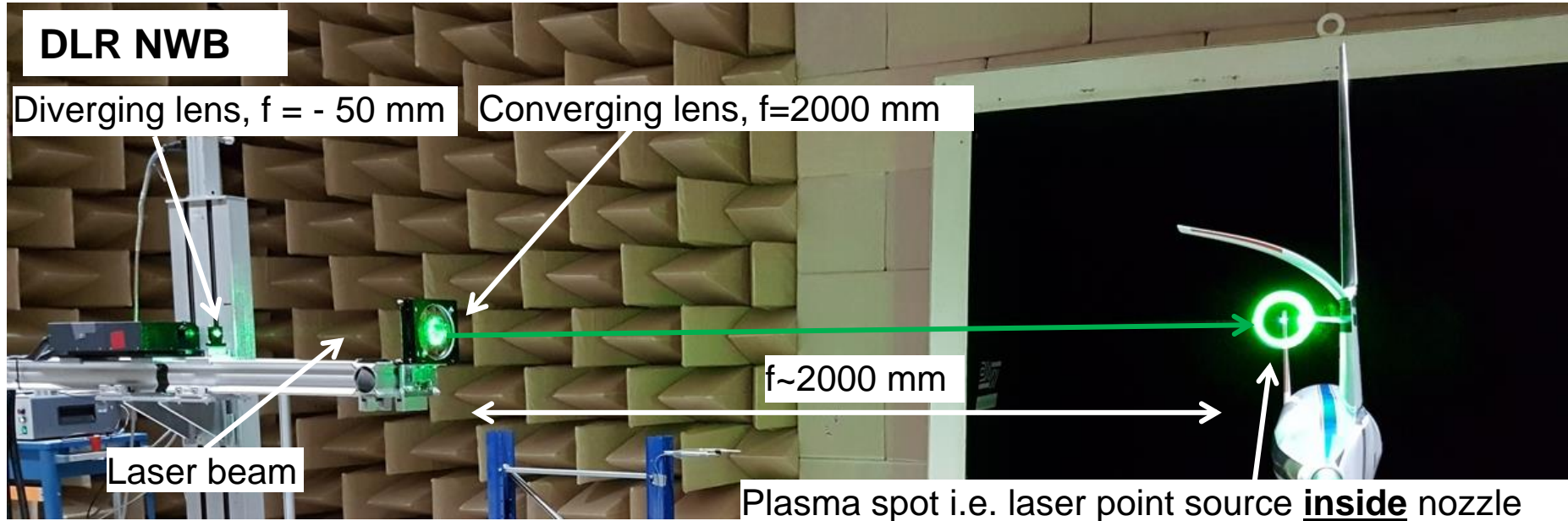
FLORIDA STATE UNIVERSITY



DLR

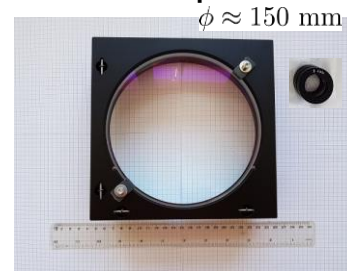
# Appendix

# Facilities - Extra



AIAA 2017-3195

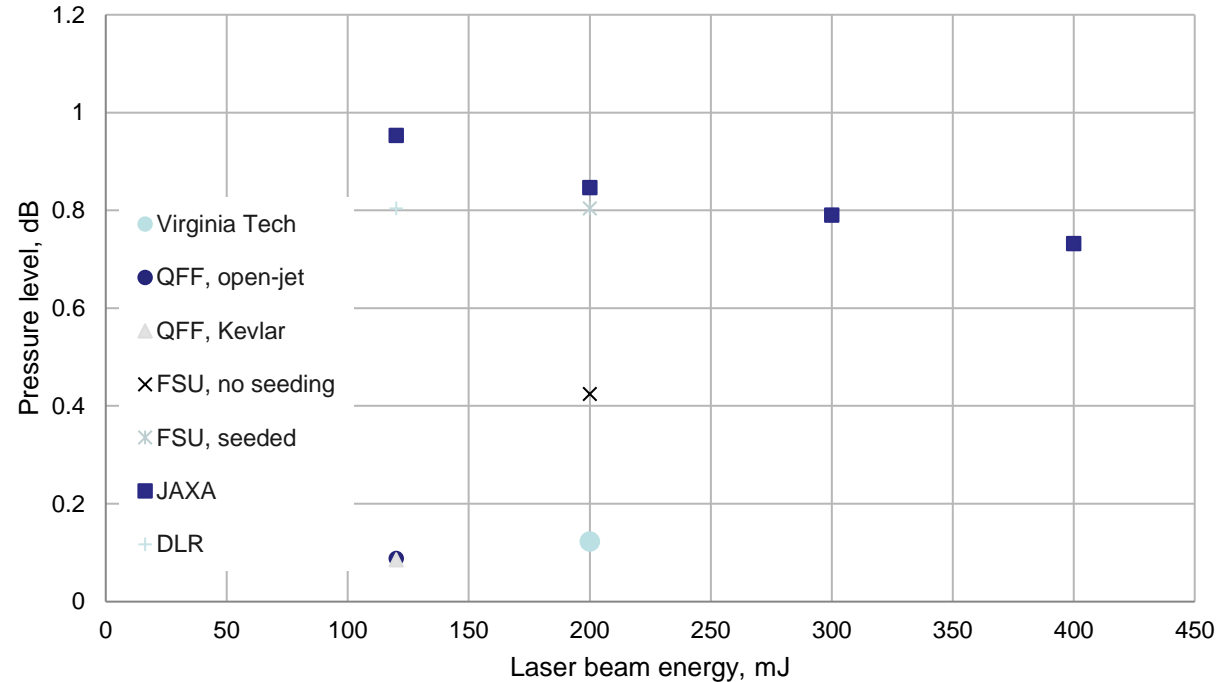
2.6' x 3.9' x 9.8'  
(0.8 m x 1.2 m x 3.0 m)



# Uncertainty analysis IV.

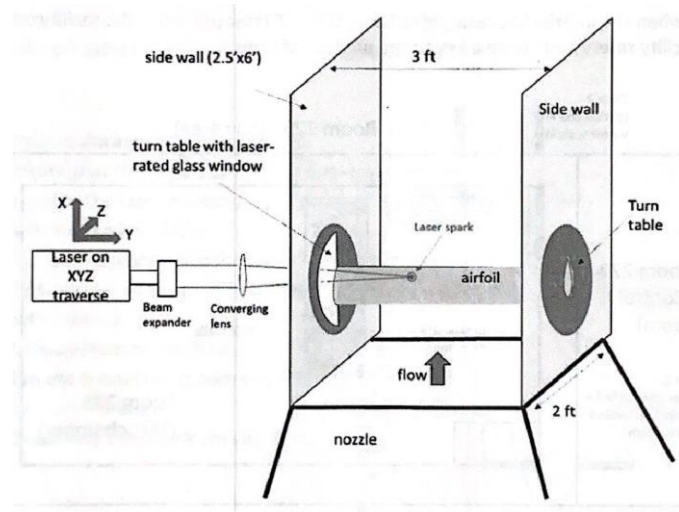
- **Pressure level uncertainty vs. laser beam energy**
- **More investigations required** to quantify laser beam energy effect on LIP acoustic signature
- Might shed light on optimal energy-density.

Pressure level uncertainty



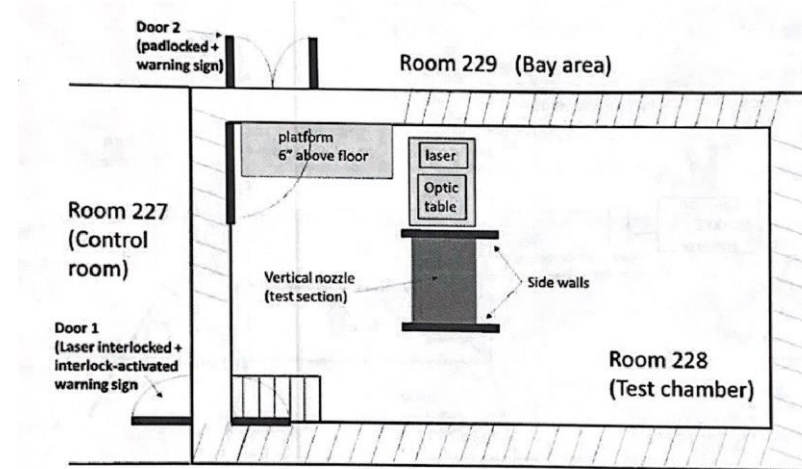
# QFF safety operating plan

- Personnel exposure
  - **Minimize personnel** in chamber
  - Laser **safety glasses** at all times
- Facility and **Interlocks**
  - Interlocks tie access door to laser power (open door = power cut off)
  - **Warning signs/lights** tied to door interlock
  - Padlocked auxiliary doors – only approved operators or facility coordinator/safety head can lock/unlock these
  - No windows from facility exterior to test section
- **Beam path** – verify sufficient beam divergence for “safe” reflections w.r.t. ablation, combustion



# QFF safety operating plan

- Normal operational procedures
  - Ensure only essential personnel is present
  - Personnel equip **safety eyewear** (if required to be in test chamber)
  - **Activate interlocks**, closing and locking doors & turning on warning lights
  - **Activate laser**
  - Start **experiments**
  - **Turn off laser** when complete
  - **Disengage interlocks**
  - Remove eyewear



# Health and safety measures: DLR

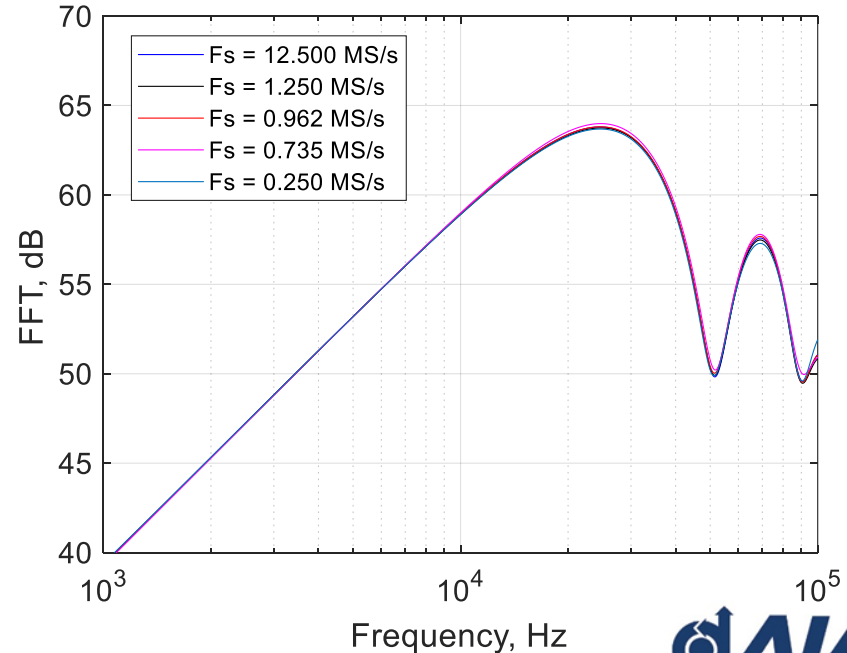
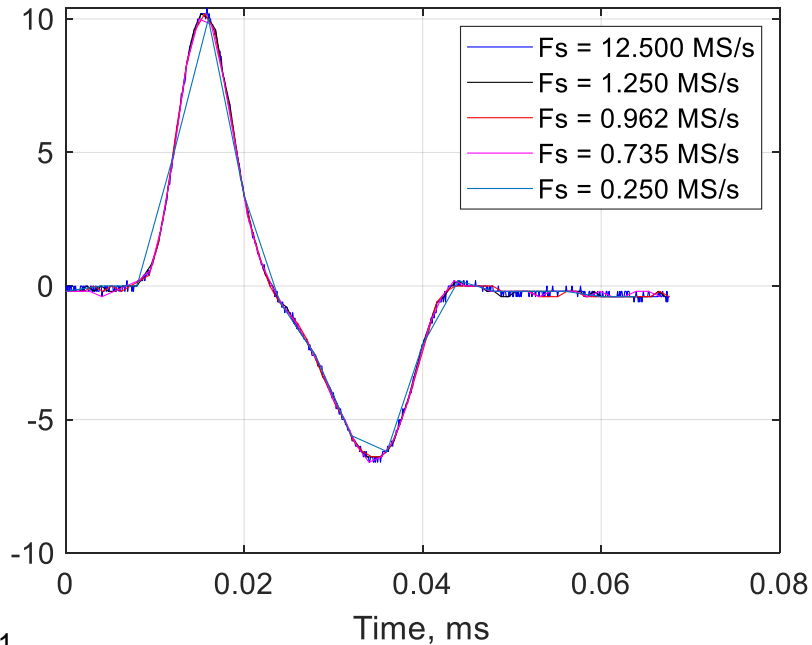
- Ensure only **essential personnel** present
- Operating personnel must receive **training** prior to using the laser
- Non-operating personnel must be **informed about safety measures** prior to tests
- Use **safety eyewear** when inside the perimeter of possible laser light emission at all times
- **Interlock** on main power line to the laser
- **Warning signs** and lights tied to laser interlock
- **No windows**
- Ensure **beam path** is cleared
- **Remote** operation of the laser possible



# Sampling rate analysis

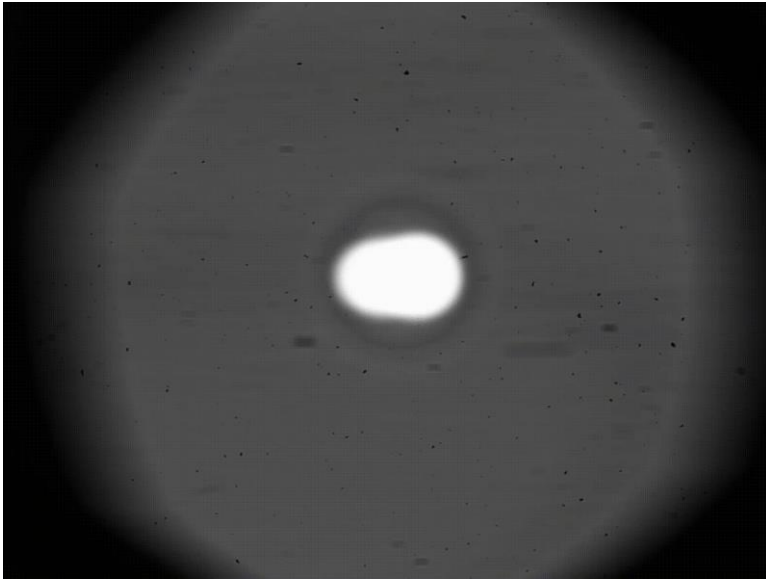
Downsampling VT's results of June 2021

Acquired using o-scope and B&K 4138 1/8" (with gridcap)



# Shadowgraph analysis of seeding effect (FSU)

Sparks without seedings



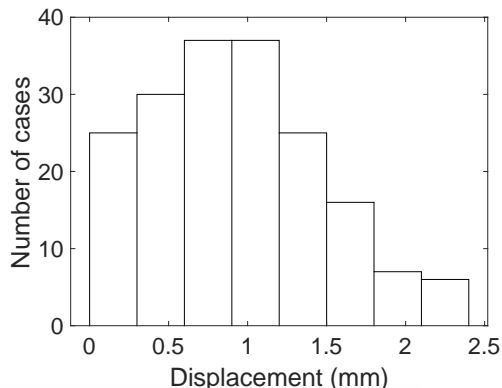
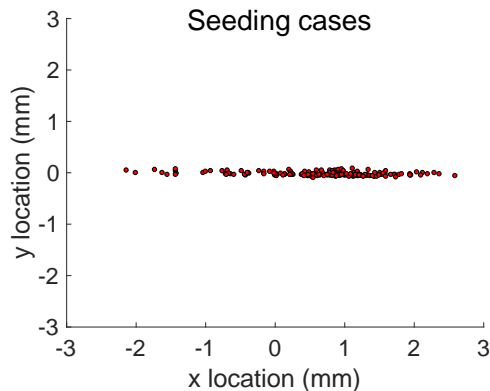
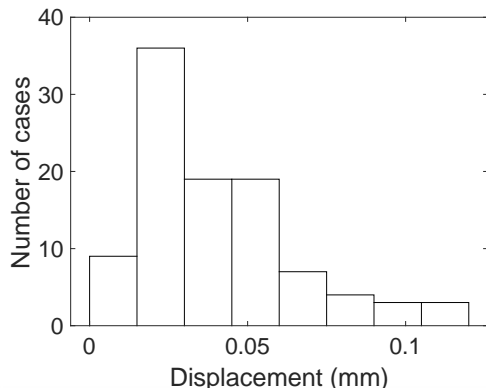
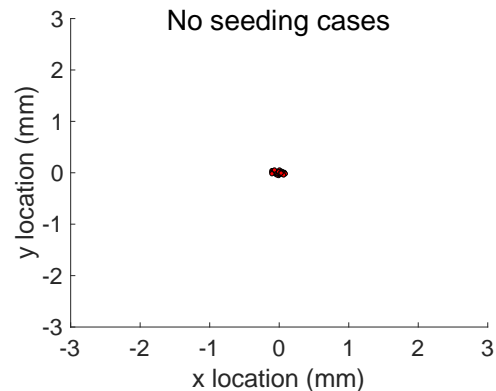
Sparks with seedings



- 'Phase locked' frames
- Averaged from 100 images per time delay
- Initial time delay at 0s.

# Shadowgraph analysis of seeding effect (FSU)

## Statistics of the spark center location



- $(x,y) = (0,0)$  represents the mean center of the no seeding cases
- 100 samples in the no seeding case vs. 180 samples in the seeding case
- Only one of the spark center is identified for the 'double-spark' in the seeding cases.
- Spark location with no seeding is significantly more consistent than that of the seeding cases.